Available online at www.ijournalse.org

Emerging Science Journal

(ISSN: 2610-9182)

Vol. 9, No. 6, December, 2025

Evaluating Sensitivity of Double EWMA Chart for ARL Under Trend SAR(1) Model and Applications

Yupaporn Areepong [1], Kotchaporn Karoon [2*]

[1] *Department of Applied Statistics, Faculty of Applied Science, King Mongkut's University of Technology North Bangkok, Bangkok, 10800, Thailand.*

[2] *Department of Mathematics, Faculty of Science, Naresuan University, Phitsanulok, 65000, Thailand.*

Abstract

The goal of this study is to offer the precise average run length (ARL) on the Double Exponentially Weighted Moving Average (double EWMA) control chart for the data underlying the first-order seasonal autoregressive ($SAR(1)_L$) with trend model. A comparison was made between the explicit formula and the computed ARL obtained using the numerical integral equation (NIE) approach, employing four quadrature methods: the midpoint, Simpson's, trapezoidal, and Boole's rules. The comparison was based on accuracy percentage (%Acc) and computation time (in seconds). The results showed that there was not much variation in accuracy between the ARL results of the explicit ARL and ARL via the NIE method. The findings indicate that the explicit ARL and NIE approaches produce very consistent accuracy values; however, the explicit formula is significantly more rapid (instantaneous compared to 1.5–26 seconds). The advantage of the double EWMA chart compared to the extended EWMA chart in identifying process changes is demonstrated, encompassing evaluations under both one-sided and two-sided setups with varied LCL values. The results are additionally corroborated by sensitivity measures (AEQL, PCI, RMI) and checked with actual durian export data, guaranteeing that the conclusions are firmly established in both simulated and empirical evidence.

Keywords:

Average Run Length;
Double EWMA Control Chart;
Extended EWMA Control Chart;
Explicit Formula;
Numerical Integral Equation.

Article History:

Received:	02	September	2025
Revised:	09	November	2025
Accepted:	21	November	2025
Published:	01	December	2025

1- Introduction

Although Statistical Process Control (SPC) has its roots in manufacturing, it is currently widely employed in a variety of industries, including healthcare, the environment, finance, education, and services. Control charts provide SPC a flexible tool for quality improvement and decision-making in a range of domains by monitoring process stability and identifying anomalous changes in mean and variance. For example, according to Freitas et al. [1], control charts were used to track the consistency of water usage, identify anomalous occurrences, and assess the effects of replacing toilets. The use of control charts to track financial flows was demonstrated by Kovarik & Klimek [2]. They used time series analysis and SPC to identify changes and guarantee stability. Khan et al. [3] introduced control charts that use neutrosophic statistics to track the quality of blood component manufacturing under uncertainty. Not long ago, Raza et al. [4] developed a control chart to track the recovery time of cancer patients in the presence of censored data in order to effectively identify variations in the average recovery time in the face of uncertainty. Nonetheless, the exponentially weighted moving average (EWMA) [5] and cumulative sum (CUSUM) [6] control charts are two popular control charts. The EWMA-type chart has also been modified in a number of research studies. When it comes to identifying even the smallest process changes, these charts have proven to be more sensitive than the typical EWMA chart. Extended

* **CONTACT**: kotchapornk@nu.ac.th

DOI: http://dx.doi.org/10.28991/ESJ-2025-09-06-026

Exponentially Weighted Moving Average (Extended EWMA) [7] and Modified Exponentially Weighted Moving Average (Modified EWMA) [8] are two examples. These control charts have been examined by numerous researchers, who have found that they are useful for identifying slight changes in processes in a variety of situations. The Double Exponentially Weighted Moving Average (Double EWMA) chart, initially presented by Shamma & Shamma [9], is a frequently used control chart. The technique was further improved by Mahmoud & Woodall [10], who showed that the DEWMA chart offers more sensitivity in identifying minute changes in process parameters.

The assumption of independent, normally distributed data is common in control charts, despite the fact that real-world data frequently displays time series patterns, including trends, seasonality, and autocorrelation. ARIMA models, which include both autoregressive (AR) and moving average (MA) components, are commonly used to handle these trends. Although white noise errors are typically thought to have a normal distribution, in certain situations they might have an exponential distribution. In this work, we examine situations in which the white noise has an exponential distribution [11].

The Average Run Length (ARL), which contains two important components, can be used to evaluate the sensitivity of control charts. The average number of observations made when the process is stable prior to a false alarm is the in-control ARL, or ARL_0. The average number of observations needed to identify a change in the process once it becomes unstable is known as the out-of-control ARL, or ARL_1. While ARL_1 should be low to guarantee the chart can promptly identify real changes, ARL_0 should ideally be high to prevent needless false alarms. Calculating ARL is a basic first step in creating a control chart. Numerous techniques have been put up to compute ARL. Brook & Evans [12] introduced the Markov approach, whereas Champ & Rigdon [13] compared the Markov Chain and Numerical Integral Equation (NIE) methods. An NIE approach that works well with real-world data that has autocorrelation and non-normal distributions was created by Peerajit (2023) [14].

Explicit formulas have been suggested as an effective means of evaluating ARL in addition to the previously listed techniques, providing a quicker and more useful substitute. It is applied widely to control charts under data when they occur as time series ARMA components under white noise exponential. Supharakonsakun [15] is one example. The modified EWMA chart was fitted to the Dow Jones composite average using a real-world dataset after a two-sided exact ARL formula was created using the general moving average (MA(q)) model. In order to determine the average run length (ARL) of modified EWMA control charts in conjunction with IMA and FIMA models for time series prediction, Ng et al. [16] put forth two explicit formulations. Energy commodity pricing data is used to illustrate the efficacy of the suggested approaches, yielding outcomes in line with experimental findings. For the double EWMA control chart, Capizzi & Masarotto [17] created explicit ARL formulations that were specific to MA(q) processes affected by exponential white noise. Their method performed well in detecting minor process changes in a variety of settings when tested using industrial commodity price data from Thailand. Karoon et al. [18] demonstrated that the double EWMA control chart using an explicit ARL formula outperforms the EWMA chart in both speed and sensitivity for detecting small shifts in autoregressive time series with exponential white noise, validated by real-world energy price data.

Horng Shiau & Ya-Chen [19] developed an explicit ARL formula for the double EWMA chart using an autoregressive model with trend and exponential white noise. The method reduced computing time when compared to the NIE methodology and was more sensitive than EWMA and CUSUM charts in detecting tiny shifts, as confirmed with digital currency data. Bualuang & Peerajit [20] developed explicit expressions and NIE for the ARL of the CUSUM chart under the ARFIX process and illustrated the proposed methodology through an economic dataset involving gold futures prices. The method, which uses Banach's theorem, outperforms the NIE approach and has excellent detection accuracy, as tested by natural gas futures data. In addition, Karoon & Areepong [21] proposed an adjusted modified EWMA control chart with an explicit ARL formula for autoregressive models with trend and exponential noise. It is faster than the NIE approach and outperforms EWMA and modified EWMA on both simulated and stock market data. Muangngam et al. [22] presented explicit ARL formulas for the extended EWMA control chart, which were applied to ARX models with exponential white noise. The method is faster than NIE (less than 0.001 seconds) and has comparable accuracy. Compared to the standard EWMA chart, the extended EWMA chart detects mean shifts more accurately, as evidenced by SCB stock prices and GDP growth data. Sunthornwat et al. [23] devised explicit ARL formulas for the HWMA control chart using autoregressive processes, which outperformed extended EWMA and CUSUM in identifying minor to moderate shifts. The chart's effectiveness was validated with economic data and measured using RMI, AEQL, and PCI measures.

Recently, Karoon & Areepong [24] reported the exact ARL solution for the new EEWMA control chart using the AR model and compared its performance to that of the regular and extended EWMA charts. The comparison was also performed on a Thai economic dataset. Peerajit (2025) [25] provided precise formulae for the EWMA chart's in-control and out-of-control ARL in a long-memory seasonal fractionally integrated moving average with exogenous variables (LSFIMAX) process. The study found that precise formulae computed ARL faster and more efficiently than numerical integral equations for power production data.

Moreover, Polyeam & Phanyaem expanded the investigation of Average Run Length (ARL) efficiency in Exponentially Weighted Moving Average (EWMA) control charts under quadratic-trend $SAR(1)_L$ [26] and $SAR(p)_L$ [27] models by developing explicit ARL formulae to supplant the numerical integral equation (NIE) technique. Their methodology was subsequently utilized to track lobar pneumonia cases in patients at Siriraj Hospital in Bangkok, Thailand. Despite these contributions signifying significant progress, a notable research deficiency persists: so far, no investigation has formulated a definitive ARL equation for the double EWMA control chart within the context of the first-order seasonal autoregressive model with trend ($SAR(1)_L$ with trend). This paper introduces the inaugural explicit Average Run Length (ARL) calculation for the double Exponentially Weighted Moving Average (EWMA) chart and systematically compares it with the NIE approach, which utilizes four composite quadrature rules: midpoint, Simpson's, trapezoidal, and Boole's. The sensitivity of the suggested chart is evaluated against the extended EWMA chart using both simulated and actual datasets, offering novel methodological insights into process monitoring among seasonal variations. The effectiveness of the suggested technique is confirmed by established performance metrics, including the Relative Mean Index (RMI), Average Extra Quadratic Loss (AEQL), and Performance Comparison Index (PCI). Additionally, a real-world dataset concerning Thailand's monthly and quarterly durian export volumes (10,000 metric tons) is utilized to assess the sensitivity of the double EWMA control chart in identifying process changes.

2- Material and Methods

2-1- Structure of Control Charts

First, Naveed et al. [7] proposed the Extended Exponentially Weighted Moving Average (extended EWMA) control chart, which was developed by Roberts [5] to monitor a process over time. It is effective for tracking and spotting minor differences in the average operation. The extended EWMA control chart can be expressed through the recursive solution shown in Equation 1 below.

$$U_t = \lambda_1 X_t - \lambda_2 X_{t-1} + (1 - \lambda_1 + \lambda_2) U_{t-1}, t = 1,2,\ldots \tag{1}$$

where λ_1 and λ_2 represent the exponential smoothing parameters with interval as $(0 < \lambda_1 \leq 1)$ and $(0 < \lambda_2 < \lambda_1)$, respectively. The initial value is a constant at $t = 0$, and U_0equal to u. The upper and lower control limits on the extended EWMA control chart are supplied by

$$UCL = \mu_0 + K\sigma\sqrt{\frac{\lambda_1^2+\lambda_2^2-2\lambda_1\lambda_2(1-\lambda_1+\lambda_2)}{2(\lambda_1-\lambda_2)-(\lambda_1-\lambda_2)^2}}, \tag{2}$$

and

$$LCL = \mu_0 - K\sigma\sqrt{\frac{\lambda_1^2+\lambda_2^2-2\lambda_1\lambda_2(1-\lambda_1+\lambda_2)}{2(\lambda_1-\lambda_2)-(\lambda_1-\lambda_2)^2}}, \tag{3}$$

respectively.

And then, the mean is denoted by μ_0, the process standard deviation by σ, and the appropriate control limit width by$K$. Let $X_t$represents a sequence of the first-order seasonal autoregressive with trend ($SAR(1)_L$ with trend) model with exponential white noise. Then, the mean of process variableX_t, which is monitored by the extended EWMA statistic, are indicated by μ_0. The variance of process variable$X_t$is showed as

$$\left(\sigma^2\left[\frac{\lambda_1^2 + \lambda_2^2 - 2\lambda_1\lambda_2(1 - \lambda_1 + \lambda_2)}{2(\lambda_1 - \lambda_2) - (\lambda_1 - \lambda_2)^2}\right]\right) \tag{4}$$

To get the stopping time of the extended EWMA control chart, use $\tau_U = inf\{t \geq 0; U_t < LCL \quad or \quad U_t > UCL\}$ where e and f are expressed as the lower and upper control limit of two-sided extended EWMA control chart.

Second, in order to effectively monitor minute changes in process parameters, Mahmoud & Woodall [10] developed the double EWMA control chart, which was first developed by Shamma & Shamma [9] by updating the traditional EWMA control chart. The statistics of the double EWMA control chart can be approximated using Equation 5:

$$\begin{aligned} &D_t = \lambda_1 E_t + (1 - \lambda_1) D_{t-1} \quad \text{and} \\ &E_t = \lambda_2 X_t + (1 - \lambda_2) E_{t-1}, \quad t = 1,2,\ldots \end{aligned} \tag{5}$$

where λ_1 and λ_2 represent exponential smoothing parameters with intervals that are $(0 < \lambda_1 \leq 1)$ and $(0 < \lambda_2 < 1)$, respectively, which is consistent with exponential smoothing parameters of extended EWMA. And then, D_t with $t =$ 0expressed as the initial value of the double EWMA statistics, and D_0equal to s. The double EWMA control chart has the following upper (UCL) and lower (LCL) control limits:

$$UCL = \mu_0 + \widehat{K}\sigma\sqrt{\frac{\lambda_1^2\lambda_2^2}{(\lambda_1-\lambda_2)^2}\left[\frac{(1-\lambda_1)^2}{1-(1-\lambda_1)^2}+\frac{(1-\lambda_2)^2}{1-(1-\lambda_2)^2}-2\frac{(1-\lambda_1)(1-\lambda_2)}{1-(1-\lambda_1)(1-\lambda_2)}\right]}, \quad (6)$$

and

$$UCL = \mu_0 - \widehat{K}\sigma\sqrt{\frac{\lambda_1^2\lambda_2^2}{(\lambda_1-\lambda_2)^2}\left[\frac{(1-\lambda_1)^2}{1-(1-\lambda_1)^2}+\frac{(1-\lambda_2)^2}{1-(1-\lambda_2)^2}-2\frac{(1-\lambda_1)(1-\lambda_2)}{1-(1-\lambda_1)(1-\lambda_2)}\right]}, \quad (7)$$

respectively.

The mean is denoted by μ_0, the process standard deviation by σ, and the appropriate control limit width by $\widehat{K}$. The mean and variance of the process variable X_t, which is utilized to produce the double EWMA statistics, μ_0 and

$$\left(\frac{\lambda_1^2\lambda_2^2}{(\lambda_1-\lambda_2)^2}\sigma^2\left[\frac{(1-\lambda_1)^2}{1-(1-\lambda_1)^2}+\frac{(1-\lambda_2)^2}{1-(1-\lambda_2)^2}-2\frac{(1-\lambda_1)(1-\lambda_2)}{1-(1-\lambda_1)(1-\lambda_2)}\right]\right), \quad (8)$$

respectively.

The stopping time of the EEWMA control chart can be determined using $\tau_D = inf\{\, t \geq 0; D_t < LCL \quad or \quad D_t > UCL\}$ where a and bThe lower and upper control limits of the two-sided double EWMA control chart are represented by a and b, respectively.

Furthermore, because they can be converted into the conventional EWMA statistic, the double EWMA and extended EWMA statistics are both equivariant. In particular, the double EWMA statistic reduces to the conventional EWMA statistic when it is set to 1. In the same way, the extended EWMA statistic becomes equal to the EWMA statistic when it is set to 0.

2-2- Derivation Approach for the Explicit ARL Formula Based on the SAR(1)$_L$ with Trend Model

To derive explicit ARL formulas, this research used a statistical method for analyzing time-series data called the trend SAR(1)$_L$ model, which stands for the first-order trend seasonal autoregressive model. Engineering and economics are two of the many fields that make use of this approach, which takes seasonal trends and patterns into account. You may examine its formulation in Equation 9.

$$X_t = \eta + \omega t + \phi_1 X_{t-1L} + \varepsilon_t \quad (9)$$

In this context, η denotes the constant of SAR(1)$_L$ with a trend model, whereas ω signifies the constant term or trend component, considered an exogenous variable to encapsulate the underlying trend or temporal aspect of the data. Here, ϕ_1 stands for the time series model's first-order coefficients, where $\phi_1 \in (-1,1)$. At this point L stands for the seasonal length; numbers 4 and 12 indicate quarterly and monthly data, respectively. Also, $\varepsilon_t \sim Exp(\beta)$ stands for the error term, which is presumed to be a continuous i.i.d. random variable created from exponential white noise. One way to represent the probability density function of ε_t is as $f(x,\beta) = \frac{1}{\beta e^{-\frac{x}{\beta}}}; \beta > 0$.

This study uses the ARL characteristics as a guide to analyze many change-point models.

$$\varepsilon_t \sim \begin{cases} Exp(\beta_0), & t = 1,2,\ldots,\Phi-1 \\ Exp(\beta_1), & t = \Phi,\Phi+1,\ldots \end{cases} \quad (10)$$

It is where the parameters β_0 and β_1 are known, with β_0 standing for the mean of the exponential distribution $\beta_1 > \beta_0$, and the ARL defined with $E_\Phi(.)$can be explained by examining the change point in Equation 10.

$$\text{ARL} = \begin{cases} \text{ARL}_0 = E_\infty(\tau), \beta = \infty & \text{(no change)} \\ \text{ARL}_1 = E_1(\tau), \beta = 1 & \text{(change)} \end{cases} \quad (11)$$

where $E_\Phi(.)$is the mean under exponential distribution $f(x,\beta)$ for a given change-point time. $\beta = \infty$ shows in-control which stands for ARL$_0$, whereas $\beta = 1$ Represents the first occurrence of a shift from β_0 to β_1 in the process, which is known as out-of-control ARL which stands for ARL_1. $\beta = \infty$ indicates in control, which stands for ARL$_0$, and $\beta = 1$ represents out of control. Stands for the initial transition from β_0 to β_1 in the process, which is called out-of-control ARL (or ARL$_1$). With a change-point at time t=1, let ε_t represent the Extended EWMA statistic. After that, the statistic from Equation 5 can be rewritten using the SAR(1)$_L$ with trend model:

$$D_t = \lambda_1(\lambda_2\{\eta + \omega t + \phi_1 X_{t-1L} + \varepsilon_t\} + (1-\lambda_2)E_{t-1}) + (1-\lambda_1)D_{t-1}. \quad (12)$$

The D_t is rearranged in this way:

$$D_t = \lambda_1\lambda_2(\eta + \omega t + \phi_1 X_{t-1L}) + \lambda_1\lambda_2\varepsilon_t + \lambda_1(1-\lambda_2)E_{t-1} + (1-\lambda_1)D_{t-1} \quad (13)$$

By substituting t =1 into D_t and considering the interval $a < D_t < b$, it follows that

$$\frac{a-(1-\lambda_1)u}{\lambda_1\lambda_2}-\frac{(1-\lambda_2)z}{\lambda_2}-y<\varepsilon_1<\frac{b-(1-\lambda_1)u}{\lambda_1\lambda_2}-\frac{(1-\lambda_2)z}{\lambda_2}-y \tag{14}$$

where D_0 and E_0 are initial values of double EWMA statistics, which are u and z, respectively. And then, $y$represents $\eta+\omega t+\phi_1 X_{t-1L}$.

When applied to a double EWMA control chart, the SAR(1)$_L$ with trend model explicit ARL formula is $D(u)$. This formula was obtained in this study by changing the Fredholm integral equation of the second kind [28].

$$D(u)=1+\int_l^h D(\lambda_1\lambda_2(y+\varepsilon_1)+(1-\lambda_1)u+\lambda_1(1-\lambda_2)z)\,g(\varepsilon_1)d\varepsilon_1 \tag{15}$$

where l and h represent $\frac{a-(1-\lambda_1)u}{\lambda_1\lambda_2}-\frac{(1-\lambda_2)z}{\lambda_2}-y$ and $\frac{b-(1-\lambda_1)u}{\lambda_1\lambda_2}-\frac{(1-\lambda_2)z}{\lambda_2}-y$, respectively.

Given that ξ is $\lambda_1\lambda_2(y+\varepsilon_1)+(1-\lambda_1)u+\lambda_1(1-\lambda_2)z$, then $\frac{d\xi}{d\varepsilon_1}=\lambda_1\lambda_2$ thus, $\frac{d\xi}{\lambda_1\lambda_2}=d\varepsilon_1$.

This expression can be rearranged as Equation 16 which is provided below. The integral variable of $D(u)$, was changed.

$$D(u)=1+\frac{1}{\lambda_1\lambda_2}\int_a^b D(\xi)\,g\left(\frac{\xi-(1-\lambda_1)u}{\lambda_1\lambda_2}-\frac{(1-\lambda_2)z}{\lambda_2}-y\right)d\xi. \tag{16}$$

To establish the existence of the ARL solution for the double EWMA control chart that is applied to the SAR(1)$_L$ with trend process, the next step involves proving Equation 5 by applying Banach's fixed-point theorem [29]. This validates the uniqueness of the solution. Detailed information regarding the technique can be found in part of the existence and uniqueness of Banach's fixed-point theorem, which corresponds to this outline.

Next step, when $\varepsilon_1\sim Exp(\beta)$. Obtaining the explicit ARL formula, which is characterized by the error terms as having an exponential distribution, can be accomplished by using the second-kind Fredholm integral equation. The formula is then modified to:

$$D(u)=1+\frac{\exp\{A+B+C\}}{\beta\lambda_1\lambda_2}\int_a^b D(\xi)\cdot exp\left\{-\frac{\xi}{\beta\lambda_1\lambda_2}\right\}d\xi \tag{17}$$

where; A, B, and C represent $\frac{(1-\lambda_1)u}{\beta\lambda_1\lambda_2}$, $\frac{(1-\lambda_2)z}{\beta\lambda_2}$, and $\frac{y}{\beta}$, respectively. Moreover, $M(u)$ equal to $exp\{A+B+C\}$.

After that, Equation 17 can be modified to the following new variables:

$$D(u)=1+\frac{M(u)}{\beta\lambda_1\lambda_2}H \tag{18}$$

and

$$H=\int_a^b D(\xi)\Omega(\xi)d\xi \tag{19}$$

When Equation 19 is replaced into Equation 17, we obtain the following:

$$H=\int_a^b\left(1+\frac{M(u)}{\beta\lambda_1\lambda_2}H\right)\Omega(\xi)d\xi=-\frac{\beta\lambda_1\lambda_2[\Omega(b)-\Omega(a)]}{1+\frac{exp\{A+B+C\}}{\lambda_1}[(\lambda_2 b)-\Omega(\lambda_2 a)]} \tag{20}$$

Replace Equation 20 with 18, Equation 21 shows the exact ARL for the double EWMA control chart under the trend SAR(P)$_L$ model after rearranging the equation

$$D(u)=1-\frac{\lambda_1\cdot exp\{A\}[\Omega(b)-\Omega(a)]}{\lambda_1\cdot exp\{-(B+C)\}+[\Omega(\lambda_2 b)-\Omega(\lambda_2 a)]} \tag{21}$$

where; $\Omega(a)$, $\Omega(b)$, $\Omega(\lambda_2 a)$, and $\Omega(\lambda_2 b)$ represent $exp\left\{-\frac{a}{\beta\lambda_1\lambda_2}\right\}$, $exp\left\{-\frac{b}{\beta\lambda_1\lambda_2}\right\}$, $exp\left\{-\frac{a}{\beta\lambda_1}\right\}$, and $exp\left\{-\frac{b}{\beta\lambda_1}\right\}$, respectively.

Further to Equation 21, β is replaced by β_0 and β_1, which signify the in-control and the out-of-control states, respectively.

2-3-Approach to ARL Using NIE Methods in the SAR(1)$_L$ with Trend Model

The SAR(1)$_L$ with trend model analysis now uses the Numerical Integral Equation (NIE) approach. Equation 16 solves m linear equations to approximate the double EWMA control chart's Average Run Length (ARL). Classical quadrature approaches, such as Midpoint (N1), Simpson's (N2), Trapezoidal (N3), and Boole's (N4) rules, provide the basis for the ARL estimates that are obtained as a result through the use of the Gauss-Legendre quadrature on the interval $a\le r_1\le\ldots\le r_m\le b$ and $r_j=(j-0.5)w_j+a$. These estimates are designated by the symbol $N(u)$. Furthermore, these approaches

are specified by a set of nodes $\{r_j, j = 0,1,2,\dots,m\}$ and a set of weights $\{w_j, j = 0,1,2,\dots,m\}$ that correspond to those nodes. In most cases, the integral is approximated by using the expression that is presented below:

$$\int_a^b w(r)\, g(r)dr \approx \sum_{j=1}^{m} w_j\, f(r_j) \tag{22}$$

When applied, the quadrature method yields the result that is presented below:

$$N(r_i) = 1 + \frac{1}{\lambda_1\lambda_2}\sum_{j=1}^{m} w_j \cdot N(r_j) \cdot g\left(\frac{r_j-(1-\lambda_1)r_i}{\lambda_1\lambda_2} - \frac{(1-\lambda_2)z}{\lambda_2} - y\right), \quad i = 1,2,\dots,m. \tag{23}$$

The system is a matrix of m linear equations, defining m to m^{th} as elements of R. The elements of matrix R as shown as follows:

$$[R_{ij}] \approx \frac{1}{\lambda_1\lambda_2} w_j \cdot g\left(\frac{r_j-(1-\lambda_1)r_i}{\lambda_1\lambda_2} - \frac{(1-\lambda_2)z}{\lambda_2} - y\right). \tag{24}$$

To summarize, the variable u is utilized instead of the variable r_j, and the numerical formulation for approximating $N(u)$ is demonstrated in Equation 25 by

$$N(u) = 1 + \frac{1}{\lambda_1\lambda_2}\sum_{j=1}^{m} w_j \cdot N(r_j) \cdot g\left(\frac{r_j-(1-\lambda_1)u}{\lambda_1\lambda_2} - \frac{(1-\lambda_2)z}{\lambda_2} - y\right), \quad i = 1,2,\dots,m. \tag{25}$$

Table 1 summarizes composite quadrature rules, including weights, based on equal subinterval widths $h = (b-a)/m$. Subsequently, $N(u)$ is substituted by N1, N2, N3, and N4, representing the Midpoint, Simpson's, Trapezoidal, and Boole's rules, respectively. Moreover, $\left(\frac{r_j-(1-\lambda_1)u}{\lambda_1\lambda_2} - \frac{(1-\lambda_2)z}{\lambda_2} - y\right)$ is demonstrated by Λ. When the node (r_j) of Midpoint quadrature rules is defined as $a + (j-0.5)h$, whereas the node (r_j) of Simpson's, Trapezoidal, and Boole's quadrature rules are determined as $a + jh$.

Table 1. The composite quadrature rules

Rules	Formulas	Weight
Midpoint	$\mathrm{N1} = 1 + \frac{1}{\lambda_1\lambda_2}\sum_{j=1}^{m} w_j \cdot N(r_j) \cdot g(\Lambda)$	h
Simpson's	$\mathrm{N2} = 1 + \frac{1}{\lambda_1\lambda_2}\sum_{j=0}^{2n} w_j \cdot N(r_j) \cdot g(\Lambda)$, where $m = 2n$	$\frac{h}{3}; j = 0,2n, \frac{4h}{3}; j = 1,\dots,2n-1, \frac{2h}{3}; j = 2,\dots,2n-2$
Trapezoidal	$\mathrm{N3} = 1 + \frac{1}{\lambda_1\lambda_2}\sum_{j=0}^{m} w_j \cdot N(r_j) \cdot g(\Lambda)$	$\frac{h}{2}; j = 0, m, h; j = 1,\dots, m-1$
Boole's	$\mathrm{N4} = 1 + \frac{1}{\lambda_1\lambda_2}\sum_{j=0}^{4n} w_j \cdot N(r_j) \cdot g(\Lambda)$, where $m = 4n$	$\frac{14h}{45}; j = 0,4n, \frac{64h}{45}; j = 1,\dots,4n-3,4n-1, \frac{24h}{45}; j = 2,\dots,4n-2, \frac{28h}{45}; j = 4,\dots,4n-4$

2-4- Verification of the Explicit ARL Formula's Existence and Uniqueness

This section uses Banach's fixed-point theorem to demonstrate the existence and uniqueness of the ARL solution, as the explicit ARL formula necessitates such proof. An operation that belongs to the class of all continuous functions is denoted by *T*, and it can be represented as follows below:

$$T(D(u)) = 1 + \frac{1}{\lambda_1\lambda_2}\int_a^b D(\xi)\, g\left(\frac{\xi-(1-\lambda_1)u}{\lambda_1\lambda_2} - \frac{(1-\lambda_2)z}{\lambda_2} - y\right) d\xi \tag{26}$$

Theorem 1 Banach's Fixed-point Theorem:

A complete metric space and the contraction mapping are supposed to be represented by the (X, D) and $T: X \to X$, respectively. Thereafter, the *T* is thought of as being unique on a fixed point. A unique solution exists for the fixed point in $T(D(u)) = D(u) \in X$.

In order to demonstrate this, let the contraction mapping for $D(u)_1, D(u)_2 \in u[a,b]$ be represented by *T*, which was found in Equation 16. Therefore, $\|T(D(u)_1) - T(D(u)_2)\| \le \Upsilon\|D(u)_1 - D(u)_2\|, D(u)_1, D(u)_2 \in X$, where Υ is a positive constant, this is the case.

Taking into consideration:

$$\begin{aligned}&\|T(D(u)_1) - T(D(u)_2)\|_\infty = \sup_{u\in[a,b]} |D(u)_1 - D(u)_2| = \sup_{u\in[a,b]} \left|\frac{\exp\{A+B+C\}}{\beta\lambda_1\lambda_2}\int_a^b (D_1(\xi) - D_2(\xi)) \cdot exp\left\{-\frac{\xi}{\beta\lambda_1\lambda_2}\right\} d\xi\right| \le \\ &\sup_{u\in[a,b]} \left|\|T(D(u)_1) - T(D(u)_2)\|_\infty \cdot \frac{\exp\{A+B+C\}}{\beta\lambda_1\lambda_2} \cdot (-\beta\lambda_1\lambda_2)\left(exp\left\{-\frac{b}{\beta\lambda_1\lambda_2}\right\} - exp\left\{-\frac{a}{\beta\lambda_1\lambda_2}\right\}\right)\right| = \|D(u)_1 - \\ &D(u)_2\|_\infty \sup_{u\in[a,b]} |\exp\{A+B+C\}| \left|exp\left\{-\frac{a}{\beta\lambda_1\lambda_2}\right\} - exp\left\{-\frac{b}{\beta\lambda_1\lambda_2}\right\}\right| \le \Upsilon\|D(u)_1 - D(u)_2\|_\infty\end{aligned} \tag{27}$$

where $\Omega = \sup_{u\in[a,b]} |\exp\{A+B+C\}| \left|exp\left\{-\frac{a}{\beta\lambda_1\lambda_2}\right\} - exp\left\{-\frac{b}{\beta\lambda_1\lambda_2}\right\}; \right| \Upsilon \in [0,1)$.

And then, A, B, and C denote $\frac{(1-\lambda_1)u}{\beta\lambda_1\lambda_2}$, $\frac{(1-\lambda_2)z}{\beta\lambda_2}$, and $\frac{y}{\beta}$, respectively.

3- The ARL Procedure for Analyzing Outcomes

One common way to measure the efficiency of a control chart is by looking at its ARL for process change detection. This study assessed how well the explicit formula and the NIE technique compute the ARL for shift monitoring. It was determined that the performance with exponential white noise could be evaluated by using the double EWMA control chart that was running on the first-order seasonal autoregressive model with trend, also known as $SAR(1)_L$ with trend. To fill that gap, this paper develops an explicit ARL formula for the double EWMA chart and compares its performance to that of the numerical integral equation (NIE) method, which uses four composite quadrature rules, namely the midpoint, Simpson's, trapezoidal, and Boole's rules. Additionally, as previously stated, "exponential white noise" describes the residual of an exponential distribution. A consequence of this is that $\delta = 0$ was shown to be a process that was in control, whereas $\delta > 0$ is an example of a process that was out of control. Using the ARL approximation, the four rules of the NIE approach are utilized to ascertain the number of division points (m), which is equal to 500 at the moment. A program called Mathematica was utilized to compute both the explicit ARL and the NIE approach to the ARL. For the purpose of evaluating Mathematica, a Windows 10 (64-bit) platform in conjunction with an Intel Core i5-8250U processor operating at 1.60–1.80 GHz and 4 GB of RAM was utilized. A concise explanation of the process is provided in the following statement (see Figure 1):

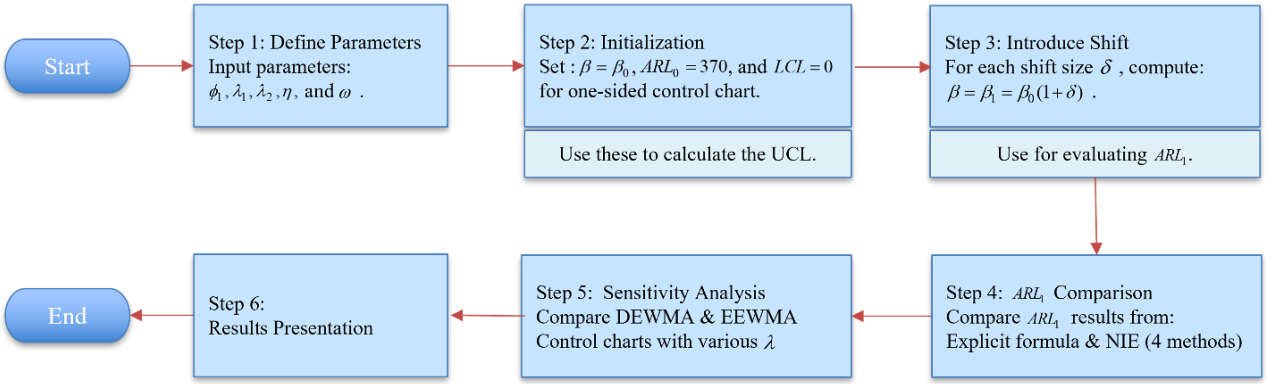

Figure 1. The procedure of ARL evaluation

4- Evaluating The Sensitivity of Control charts

For the in-control scenario, the simulated data is frequently given with ARL_0 = 370, allowing the beginning parameters to be explored at $\beta_0 = 1$. On the other hand, $\beta_1 = \beta_0(1+\delta)$ is researched in the out-of-control scenario and computed to determine shift sizes. At the interval [0, b], the lower and higher control limits are investigated. First, the ARL was evaluated using the explicit formula and the NIE method, and the capability of the methods was compared with the percentage accuracy (%Acc). In this context, the terms "*Explicit*" and "*NIE*" will be used to denote the ARL values that are obtained from the explicit formula and the NIE technique, respectively, through Equations 20 and 21. The percentage accuracy (%Acc) are calculated using Equation 28.

$$\%\text{Acc} = 100 - \left(\left|\frac{Explicit-NIE}{Explicit}\right| \times 100\%\right) \quad (28)$$

These results, described in Table 2, are based on the trend $SAR(1)_4$ model. Following that, the process was carried out on a one-sided double EWMA control chart with the interval [0, UCL] and known parameters; $\eta = \omega = 0.4, \phi_1 = 0.1, \lambda_1 = 0.10, \lambda_2 = 0.05$,0.10, and 0.15. Moreover, ARL_0 was set to 370. The ARL_1 values were then obtained for shift sizes (δ) of 0.0005, 0.001, 0.0025, 0.005, 0.01, 0.05, 0.1, and 0.5. Both methods demonstrate about the same amount of accuracy, since the percentage is close to 100% in all cases. However, in each and every instance, the precise formula produces results in a manner that is nearly instant as well. While the NIE approach and the four quadrature rules produce ARL values, the response times for these values vary greatly. A response time of about 1.4 to 1.6 seconds is observed under the midpoint rule and trapezoidal rule, the quickest of the four quadrature rules; a response time of about 5.8 to 6.4 seconds is observed under Simpson's rule; and a response time of about 23.4 to 25.7 seconds is observed under Boole's rule. The current results validate that the ARL values derived from the explicit formula and the four NIE rules are extremely constant across all shift magnitudes, which is similar to the study of Polyeam & Phanyaem [27], which investigated ARL efficiency in EWMA charts under quadratic-trend SAR models. The midpoint and trapezoidal rules take a little longer to process, but the explicit formula clearly gives a computational benefit. A 64-bit Windows 10

machine with an Intel Core i5-8250U CPU (1.60–1.80 GHz) and 4 GB of RAM was used to test each strategy. While hardware specs have no effect on the explicit formula, CPU performance has an impact on the NIE approaches' calculation time. Thus, the explicit ARL formula is advantageous, since it offers accuracy akin to NIE approaches while significantly decreasing computing time, an essential consideration for real-time monitoring.

4-1- Evaluating the Sensitivity of the Control Chart Obtained by Simulated Data

The average run length (ARL) calculated using the explicit formula for one-sided double EWMA was compared to the one-sided extended EWMA chart, which had various parameters set as underdetermined. This comparison was based on a simulated observation model using the trend $SAR(1)_4$ model over the interval [0,UCL], with different values for $\lambda_1$and λ_2, along with known parameters $\eta = 0.1, \omega = 0.6, \phi_1 = 0.5$. This comparison was carried out in this section. And then, for the two-sided double EWMA settings, a comparison was made between the two-sided extended EWMA chart with various parameter settings. The trend $SAR(1)_{12}$ model was derived for the interval [LCL, UCL] with $\lambda_1 = 0.15$, and λ_2 had various and known parameters; $\eta = 0, \omega = 0.5, \phi_1 = 0.5$. For the purpose of representing the in-control scenario, the simulated data is often created with an ARL_0 value of 370.

In addition to the ARL, this research employs three additional tools to assess the sensitivity of control charts and verify their efficacy: the Average Extra Quadratic Loss (AEQL), the Performance Comparison Index (PCI), and the relative mean index (RMI). In the research conducted by Karoon & Areepong [24], the Equation 28 that illustrates the procedure for computing AEQL can be found.

$$\text{AEQL} = \frac{1}{\Delta}\sum_{\delta_i=\delta_{min}}^{\delta_{max}\Sigma}\left(\delta_i{}^2 \times \left(1 - \frac{\lambda_1 \cdot exp\{A\}\left[exp\left\{-\frac{b}{\beta_0(1+\delta_i)\lambda_1\lambda_2}\right\} - exp\left\{-\frac{a}{\beta_0(1+\delta_i)\lambda_1\lambda_2}\right\}\right]}{\lambda_1 \cdot exp\{-(\text{B+C})\} + \left[exp\left\{-\frac{b}{\beta_0(1+\delta_i)\lambda_1}\right\} - exp\left\{-\frac{a}{\beta_0(1+\delta_i)\lambda_1}\right\}\right]}\right)\right) \tag{28}$$

where the magnitude of the process shift that is being monitored by the control chart is denoted by the δ_i . It is the total number of shift values that range from point δ_{min} to point δ_{max} that is represented by the symbol Δ. According to the findings of this investigation, Δ was defined as eight incremental steps that were evenly dispersed from 0.0005 to 0.5. In comparison to the other charts that were assessed, this control chart has the lowest AEQL, which indicates that it has a greater capacity to identify shifts in the process.

Next, the Performance Comparison Index (PCI) is computed by using the AEQL values present in each control chart as the basis for the calculation. The PCI is the ratio of the AEQL of a control chart to the AEQL of the lowest chart. The performance of various control charts can be compared using this standardized base, which presents a basis for comparison. In Equation 29, the PCI can be stated mathematically as follows:

$$\text{PCI} = \frac{\text{AEQL}}{\text{AEQL}_{\text{Lowest}}} \tag{29}$$

A PCI value of 1 is often indicative of optimal control chart performance, which is defined by the rapid detection of process alterations and a low rate of false alarms.

Furthermore, the relative mean index (RMI) is utilized specifically for the purpose of evaluating the performance of a one-sided and two-sided double EWMA control chart on different bound control limits [LCL, UCL]. Additionally, the RMI is utilized to evaluate the comparative performance of the one-sided extended EWMA control chart under different λ_1 and λ_2 conditions and different parameters. Our ability to compute the RMI is as follows:

$$\text{RMI} = \frac{1}{n}\sum_{i=1}^{n}\left(\frac{\text{ARL}_i(row) - \text{ARL}_i(smallest)}{\text{ARL}_i(row)}\right) \tag{30}$$

$\text{ARL}_i(\boldsymbol{row})$ represents the ARL of the control chart in relation to the shift size of row *i*, and $\text{ARL}_i(\boldsymbol{smallest})$ represents the smallest ARL of all of the control chart for the shift size of row *i*. Given that the RMI value of the control chart was the lowest, it can be deduced that it exhibited the highest level of performance when it came to change detection.

The examination of lower and upper control limits is performed within the interval [LCL, UCL] for both the one-sided control chart and two-sided control chart. The initial parameters used in the simulated study are summarized in Tables 3 and 4. For clarity, the term "DEWMA" denotes the double EWMA control chart, while "EEWMA" refers to the extended EWMA control chart, as illustrated in the tables and figures of this article. The results for the one-sided control charts under the trend $SAR(1)_4$ model are presented in Table 3. While the results for the two-sided control charts under the trend $SAR(1)_{12}$ model are presented in Table 4. Moreover, ARL_0 was fixed at 370, and the ARL_1 values were computed for shift sizes (δ) of 0.0005, 0.001, 0.0025, 0.005, 0.01, 0.05, 0.1, and 0.5. The smoothing parameters λ_1 was chosen from a predefined set (0.05, 0.1, 0.15) based on their common use in EWMA-related studies. And then, the smoothing parameters λ_2 of extended EWMA and double EWMA control charts were established based on the assumptions of the control charts referenced in Naveed et al. [7] and Mahmoud & Woodall [10], respectively.

Table 2. ARL values of the explicit formula and four methods of NIE technique for the trend SAR(1)$_4$ model on one-sided double EWMA chart with interval [0,UCL] and known parameters; $\lambda_1 = 0.10, \eta = \omega = 0.4, \phi_1 = 0.1$ at $ARL_0 = 370$

The smoothing parameters and UCL as λ_1, λ_2 and b	Shift sizes (δ)	Explicit Formula (CPU Time)	NIE techniques (CPU Time, Acc(%))			
			Midpoint	Simpson's	Trapezoidal	Boole's
$\lambda_1 = 0.10$, $\lambda_2 = 0.10$, $b = 0.00105684$	0	370.1002 (<0.1)	370.1002 (1.578, 100)	370.1002 (5.953, 100)	370.1002 (1.516, 100)	370.1002 (23.954, 100)
	0.0005	227.5085 (<0.1)	227.5085 (1.547, 100)	227.5085 (6.016, 100)	227.5085 (1.5, 100)	227.5085 (24.406, 100)
	0.001	164.3549 (<0.1)	164.3548 (1.453, 100)	164.3549 (5.953, 100)	164.3549 (1.484, 100)	164.3549 (24.015, 100)
	0.0025	89.8929 (<0.1)	89.8929 (1.485, 100)	89.8929 (5.937, 100)	89.8929 (1.453, 100)	89.8929 (24.125, 100)
	0.005	51.4522 (<0.1)	51.4522 (1.641, 100)	51.4522 (6.297, 100)	51.4522 (1.594, 100)	51.4522 (25.562, 100)
	0.01	27.9861 (<0.1)	27.9861 (1.577, 100)	27.9861 (6.109, 100)	27.9861 (1.531, 100)	27.9861 (23.969, 100)
	0.05	6.5759 (<0.1)	6.5759 (1.485, 100)	6.5759 (6.046, 100)	6.5759 (1.547, 100)	6.5759 (24.187, 100)
	0.1	3.7178 (<0.1)	3.7178 (1.563, 100)	3.7178 (5.937, 100)	3.7178 (1.531, 100)	3.7178 (24.016, 100)
	0.5	1.4449 (<0.1)	1.4449 (1.469, 100)	1.4449 (6.078, 100)	1.4449 (1.547, 100)	1.4449 (24.578, 100)
$\lambda_1 = 0.10$, $\lambda_2 = 0.05$, $b = 0.000117412$	0	370.0066 (<0.1)	370.0066 (1.453, 100)	370.0066 (6.047, 100)	370.0066 (1.562, 100)	370.0066 (25.328, 100)
	0.0005	196.3984 (<0.1)	196.3984 (1.485, 100)	196.3984 (5.953, 100)	196.3984 (1.515, 100)	196.3984 (24.266, 100)
	0.001	133.8188 (<0.1)	133.8188 (1.546, 100)	133.8188 (6.032, 100)	133.8188 (1.546, 100)	133.8188 (23.938, 100)
	0.0025	68.6398 (<0.1)	68.6398 (1.484, 100)	68.6398 (5.907, 100)	68.6398 (1.484, 100)	68.6398 (24.719, 100)
	0.005	38.1099 (<0.1)	38.1099 (1.672, 100)	38.1099 (6.407, 100)	38.1099 (1.562, 100)	38.1099 (26.078, 100)
	0.01	20.4029 (<0.1)	20.4029 (1.547, 100)	20.4029 (5.937, 100)	20.4029 (1.515, 100)	20.4029 (24.032, 100)
	0.05	4.8286 (<0.1)	4.8286 (1.516, 100)	4.8286 (6.094, 100)	4.8286 (1.515, 100)	4.8286 (25.125, 100)
	0.1	2.7981 (<0.1)	2.7981 (1.531, 100)	2.7981 (5.875, 100)	2.7981 (1.484, 100)	2.7981 (24.016, 100)
	0.5	1.2338 (<0.1)	1.2338 (1.500, 100)	1.2338 (5.906, 100)	1.2338 (1.516, 100)	1.2338 (24.422, 100)
$\lambda_1 = 0.10$, $\lambda_2 = 0.15$, $b = 0.002622887$	0	370.0266 (<0.1)	370.0266 (1.516, 100)	370.0266 (6, 100)	370.0266 (1.453, 100)	370.0266 (23.781, 100)
	0.0005	239.3917 (<0.1)	239.3917 (1.548, 100)	239.3917 (5.984, 100)	239.3917 (1.484, 100)	239.3917 (23.938, 100)
	0.001	177.0430 (<0.1)	177.0430 (1.499, 100)	177.0430 (5.969, 100)	177.0430 (1.515, 100)	177.0430 (24.704, 100)
	0.0025	99.6035 (<0.1)	99.6035 (1.531, 100)	99.6035 (5.922, 100)	99.6035 (1.484, 100)	99.6035 (23.468, 100)
	0.005	57.8470 (<0.1)	57.8470 (1.501, 100)	57.8470 (5.906, 100)	57.8470 (1.516, 100)	57.8470 (23.718, 100)
	0.01	31.7289 (<0.1)	31.7289 (1.61, 100)	31.7289 (6.266, 100)	31.7289 (1.563, 100)	31.7289 (25.719, 100)
	0.05	7.4667 (<0.1)	7.4667 (1.515, 100)	7.4667 (6.094, 100)	7.4667 (1.531, 100)	7.4667 (23.954, 100)
	0.1	4.1927 (<0.1)	4.1927 (1.5, 100)	4.1927 (6.031, 100)	4.1927 (1.5, 100)	4.1927 (24.094, 100)
	0.5	1.5628 (<0.1)	1.5628 (1.516, 100)	1.5628 (6.078, 100)	1.5628 (1.515, 100)	1.5628 (24.297, 100)

Table 3. ARL_1 values of the explicit formula for the trend $SAR(1)_4$ model on one-sided double EWMA and extended EWMA charts for interval [0,UCL] with various $\lambda_1$and λ_2, and known parameters; $\eta = 0.1, \omega = 0.6, \phi_1 = 0.5$ at $ARL_0 = 370$

λ_1	Control Chart	EEWMA		DEWMA			
		EEWMA-1	EEWMA-2	DEWMA-1	DEWMA-2	DEWMA-3	DEWMA-4
	λ_2	$\lambda_2 = 0.2\lambda_1$	$\lambda_2 = 0.8\lambda_1$	$\lambda_2 = 0.6\lambda_1$	$\lambda_2 = \lambda_1$	$\lambda_2 = 2\lambda_1$	$\lambda_2 = 3\lambda_1$
0.05	UCL / (δ)	0.031904	0.0195257	0.00000352746	0.0000434581	0.000390152	0.00096616
	0.0005	272.97	258.85	160.98	190.98	220.57	231.79
	0.001	216.30	199.06	103.01	128.84	157.20	168.87
	0.0025	133.51	117.80	49.74	65.42	84.65	93.29
	0.005	81.77	70.37	26.94	36.16	48.08	53.67
	0.01	46.39	39.27	14.27	19.32	26.04	29.28
	0.05	11.14	9.33	3.47	4.59	6.12	6.88
	0.1	6.19	5.20	2.10	2.67	3.48	3.88
	0.5	2.10	1.84	1.10	1.21	1.39	1.49
	AEQL	0.078	0.068	0.038	0.043	0.050	0.054
	PCI	2.034	1.765	1.000	1.121	1.310	1.412
	RMI	1.606	1.265	0.000	0.268	0.612	0.774
0.10	UCL / (δ)	0.0646424	0.0391278	0.000172135	0.000781827	0.003325165	0.00641999
	0.0005	274.25	259.03	200.22	220.71	238.15	244.44
	0.001	217.92	199.29	137.35	157.38	175.70	182.58
	0.0025	135.05	118.01	70.94	84.79	98.55	104.00
	0.005	82.93	70.51	39.51	48.17	57.15	60.80
	0.01	47.12	39.36	21.19	26.09	31.32	33.48
	0.05	11.32	9.35	5.01	6.13	7.37	7.89
	0.1	6.28	5.21	2.89	3.48	4.14	4.42
	0.5	2.12	1.84	1.25	1.39	1.55	1.62
	AEQL	0.079	0.068	0.045	0.050	0.057	0.059
	PCI	1.755	1.510	1.000	1.121	1.262	1.324
	RMI	0.914	0.649	0.000	0.179	0.365	0.442

From Table 3, $\lambda_1 = 0.05,0.10$ was the coefficient that was computed based on this experiment. And then, λ_2 is set to 0.2, and 0.8 times that of λ_1 for the extended EWMA chart, whereas λ_2 is set to 0.6, 1, 2, and 3 times that of λ_1 for the double EWMA chart. After doing the research, it was discovered that the explicit ARL that was accomplished by the double EWMA control chart was superior to that of the extended EWMA chart in a number of different smoothing parameter settings. The double EWMA chart with defined $\lambda_2 = 0.6\lambda_1$ displayed improved performance in each of the cases of the smoothing parameters λ_1. λ_2 that is set to a lower value than λ_1 or a lower λ_2 can reduce the ARL_1 value and increase the performance of chart change detection better than charts that are set to higher values of λ_2. This is a significant and remarkable discovery on the part of the researchers. The smoothing parameters $\lambda_1 = 0.15$ and λ_2, which is defined the same as λ_2 shown in Table 2, were used to define the two-sided EWMA and extended EWMA control charts. Then, the LCL values were set to 0.005, 0.01, 0.03, and 0.05.

From Table 4, the results indicated that the double EWMA chart with defined $\lambda_2 = 0.6\lambda_1$ also displayed improved performance in each of the cases of the smoothing parameters λ_1. When compared to control charts that are set to higher values of λ_2, charts with lower λ_2 allow for a reduction in the ARL_1 value and an improvement in the efficacy of chart change detection. Furthermore, the control limit (LCL) was initially fixed at 0.005 to evaluate sensitivity, which was the lowest LCL in this research, it demonstrated the most sensitivity for detecting changes in the process. In addition, the AEQL and RMI values of the double EWMA control chart with defined $\lambda_2 = 0.6\lambda_1$ expressed the lowest value in all cases, which is evidence that the double EWMA control chart is efficient in its sensitivity. On the other hand, the PCI values showed that the value is equal to 1, which indicated that the chart outperformed other control charts with other defined conditions.

The results of this investigation, illustrated in Tables 3 and 4, demonstrate the efficacy of sensitivity in identifying changes. This objective is achieved by employing a graph that depicts the correlation between ARL_1 levels and shift sizes, alongside control charts as delineated by the specific conditions in Figures 2 and 3. The efficacy of the double EWMA control chart with specified sensitivity performance was validated.

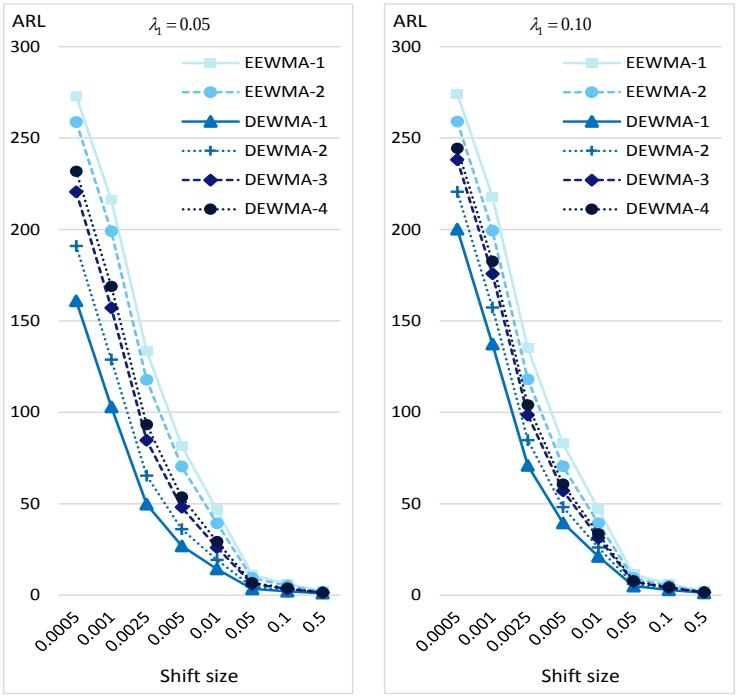

(a) (b)

Figure 2. **ARL_1 values of explicit formula for one-sided double EWMA and extended EWMA charts under various λ_2 with λ_1 equal to (a) 0.05 and (b) 0.10**

Table 4. **ARL_1 values of the explicit formula for the trend $SAR(1)_{12}$ model on two-sided double EWMA and extended EWMA charts for interval [LCL,UCL] with $\lambda_1 = 0.15$ and various λ_2, and known parameters; $\eta = 0, \omega = 0.5, \phi_1 = 0.5$ at $ARL_0 = 370$**

LCL	Control Chart	EEWMA		DEWMA			
		EEWMA-1	EEWMA-2	DEWMA-1	DEWMA-2	DEWMA-3	DEWMA-4
	λ_2	$\lambda_2 = 0.2\lambda_1$	$\lambda_2 = 0.8\lambda_1$	$\lambda_2 = 0.6\lambda_1$	$\lambda_2 = \lambda_1$	$\lambda_2 = 2\lambda_1$	$\lambda_2 = 3\lambda_1$
0.005	UCL / (δ)	0.1266325	0.0770047	0.00615731	0.00869526	0.0170756	0.0263555
	0.0005	280.70	262.17	194.66	222.01	243.15	250.03
	0.001	226.16	203.07	132.17	158.65	181.07	188.90
	0.0025	143.10	121.37	67.62	85.73	102.77	109.20
	0.005	89.03	72.92	37.57	48.82	59.99	64.38
	0.01	51.04	40.86	20.19	26.53	33.03	35.65
	0.05	12.36	9.75	4.92	6.34	7.84	8.46
	0.1	6.85	5.45	2.92	3.65	4.42	4.75
	0.5	2.28	1.92	1.33	1.48	1.66	1.73
AEQL		0.085	0.071	0.047	0.053	0.060	0.063
PCI		1.797	1.497	1.000	1.134	1.281	1.344
RMI		1.092	0.741	0.000	0.234	0.465	0.556
0.01	UCL / (δ)	0.132152	0.0820821	0.01122451	0.01382352	0.0222853	0.031603
	0.0005	278.92	259.68	166.91	205.78	235.72	245.20
	0.001	223.83	200.13	108.00	142.71	172.94	183.47
	0.0025	140.76	118.79	52.80	74.64	96.39	104.76
	0.005	87.25	71.10	28.84	41.89	55.75	61.36
	0.01	49.90	39.75	15.46	22.63	30.55	33.86
	0.05	12.08	9.50	3.96	5.52	7.30	8.06
	0.1	6.71	5.32	2.47	3.26	4.17	4.56
	0.5	2.26	1.90	1.27	1.43	1.62	1.70

AEQL		0.084	0.070	0.044	0.051	0.059	0.062
PCI		1.885	1.569	1.000	1.149	1.322	1.398
RMI		1.525	1.092	0.000	0.340	0.693	0.836
	UCL / (δ)	0.154251	0.1023912	0.031533377	0.03438101	0.04315963	0.0526209
0.03	0.0005	271.36	249.63	73.92	140.89	204.00	225.14
	0.001	214.23	188.43	41.48	87.32	141.00	161.91
	0.0025	131.54	108.84	18.36	41.20	73.53	88.1731
	0.005	80.35	64.18	9.92	22.29	41.24	50.44
	0.01	45.54	35.58	5.54	12.00	22.32	27.52
	0.05	11.03	8.55	1.96	3.31	5.53	6.67
	0.1	6.19	4.85	1.50	2.20	3.31	3.89
	0.5	2.18	1.83	1.13	1.28	1.50	1.61
AEQL		0.080	0.067	0.038	0.044	0.053	0.058
PCI		2.114	1.753	1.000	1.160	1.403	1.524
RMI		4.500	3.494	0.000	0.869	2.088	2.653
	UCL / (δ)	0.1763845	0.1226994	0.0519195954	0.055018632	0.06409476	0.0736854
0.05	0.0005	263.23	239.08	26.55	85.95	171.39	203.97
	0.001	204.35	176.69	14.25	49.03	111.78	140.96
	0.0025	122.57	99.39	6.44	21.88	55.10	73.51
	0.005	73.85	57.80	3.76	11.79	30.24	41.24
	0.01	41.52	31.82	2.40	6.51	16.28	22.33
	0.05	10.08	7.70	1.31	2.18	4.25	5.56
	0.1	5.72	4.44	1.17	1.63	2.69	3.34
	0.5	2.10	1.76	1.06	1.18	1.40	1.53
AEQL		0.077	0.064	0.035	0.040	0.049	0.054
PCI		2.188	1.810	1.000	1.132	1.392	1.542
RMI		10.850	8.601	0.000	1.512	4.568	6.226

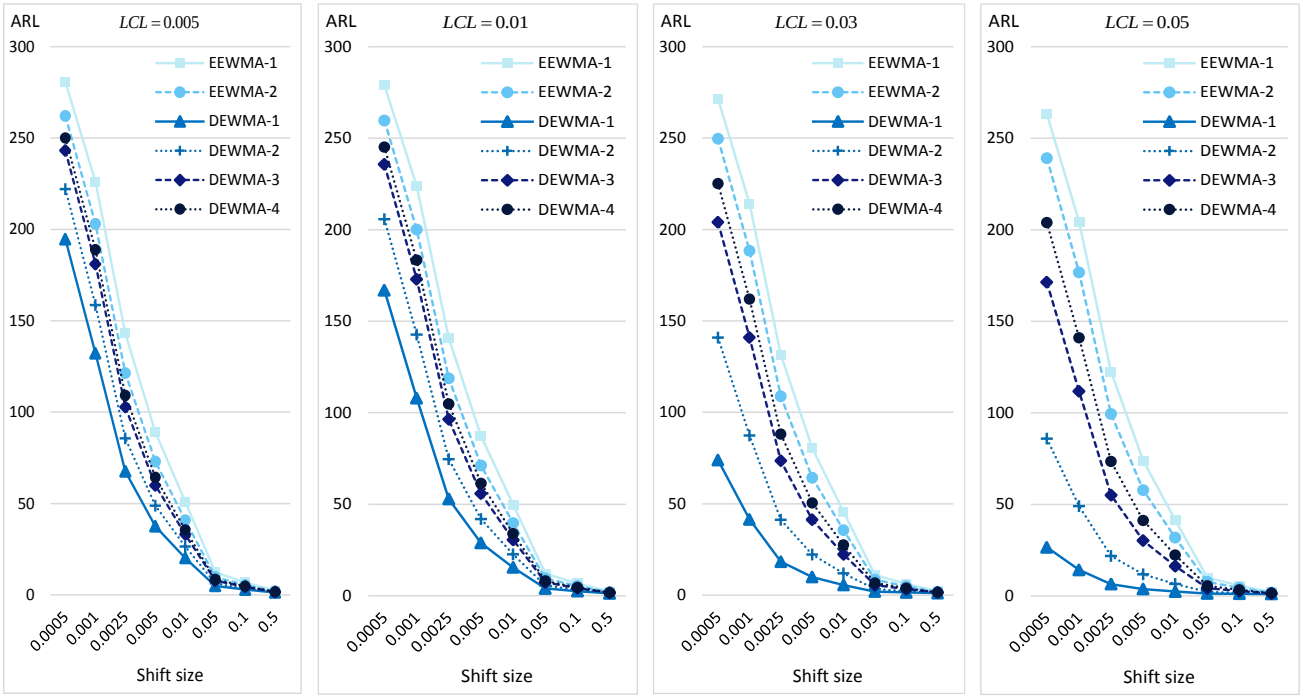

(a) (b) (c) (d)

Figure 3. ARL_1 values of explicit formula for two-sided double EWMA and extended EWMA charts with λ_1= 0.15 through various λ_2 and LCL defined as (a) 0.005, (b) 0.01, (c) 0.03, and (d) 0.05

4-2- Evaluating the Sensitivity of the Control Chart Obtained by Real-Life Data

Durian is considered one of the most economically valued tropical fruits in Thailand, and it plays an important role in producing revenue from exports. The demand is from all over the world, particularly from China and ASEAN countries. It has been gradually increasing, making the monitoring of export quantities crucial for reflecting production capacity, seasonal fluctuations, and market dynamics. The importance of the volume of durian exports can be demonstrated in a number of different ways: Export numbers are an important metric for gauging market trends, consumer demand, and the growth potential of the agricultural sector in Thailand. Agriculture and Production: Data such as this assists in the planning of activities such as harvesting, growing, and distribution in accordance with market demands and seasonal circumstances. Policy and strategic planning: By analyzing export quantities, government agencies and entrepreneurs are able to create successful trade policies and strategies that respond to the ever-changing circumstances of the global market in a timely manner. Research and Development: Data exported in time-series form is a good foundation for predicting models and examining the factors that affect market volatility. Therefore, the examination of durian export volumes not only illustrates the capabilities and potential of Thailand's fruit industry, but it also contributes to driving the national economy, advancing sustainable agricultural development, and increasing the country's competitiveness in the worldwide market. A consequence of these findings is that fluctuations in their pricing have the potential to impact decisions about monetary policy, investment behavior, and the overall stability of the economy.

Data from durian exports that have been recorded on a quarterly and monthly basis are utilized in this study (with the unit of measurement being 10,000 metric tons). An actual data analysis was carried out utilizing the trend $SAR(1)_{12}$ model with monthly observations and the trend $SAR(1)_4$ model with quarterly observations. In this study, two case studies were investigated in which the double EWMA control chart was utilized, and its performance was compared to that of the extended EWMA control chart in a variety of circumstances. Covering the time frame between January 2015 and April 2025, the dataset comprises 124 observations of the volume of durian exports on a monthly basis. Meanwhile, the dataset has 97 observations of the volume of durian exports on a quarterly basis, covering the period from Q1, 2001 to Q1, 2025. On June 4, 2025, data was gathered from these time series extracted from the internet from the website: https://app.bot.or.th/BTWS_STAT/statistics/BOTWEBSTAT.aspx?reportID=979&language=TH.

The trend $SAR(1)_L$ model (L=4 for quarterly datasets, L=12 for monthly datasets) was fitted to the real data using SPSS, and the calculated coefficients are shown in Eq. (16) and Eq. (17) for the trend $SAR(1)_4$ and trend $SAR(1)_{12}$ models, respectively, and then we are in the selection process. Two metrics were utilized: the Root Mean Squared Error (RMSE) values are so little, such as 4.062 and 4.755, respectively. To determine if the residuals adhere to an exponential distribution, the analysis involved the evaluation and application of the Kolmogorov–Smirnov (K–S) test. The data were checked under the $SAR(1)_L$ model with exponential white noise. Prior to analysis, the time series were standardized to have mean zero and variance one. The goodness-of-fit test produced results that led to the acceptance of both null hypotheses, suggesting that the residuals adhere to an exponential distribution. Its residual is that shown in both datasets that is also shown in Equations 31 and 32 too.

The following is how the trend $SAR(1)_4$ model was derived:

Dataset 1: Dataset of quarterly durian export volume (Unit: 10,000 Metric Tons). It was determined as trend $SAR(1)_4$ model, the equation is presented as follows:

$$X_t = 0.209t + 0.958X_{t-4} + \varepsilon_t \tag{31}$$

where $\varepsilon_t \sim Exp(3.13498)$.

Table 5, the findings indicate that the double EWMA chart ($\lambda_2 = 0.6\lambda_1$) exhibited better performance in all of the cases in which the smoothing parameters λ_1 and λ_2 were set to a value that was lower than λ_1. It was also determined that reducing λ_2 can improve the performance of the chart change detection by decreasing the ARL_1 value, as compared to charts that are set to higher values of λ_2. The double EWMA control chart that was defined with $\lambda_2 = 0.6\lambda_1$ indicated the lowest value for the AEQL and RMI in all of the different scenarios. This is evidence that the double EWMA control chart is effective in its sensitivity. The PCI values, on the other hand, demonstrated that they were equal to 1. This data suggested that the chart performed better than other control charts that had different stated circumstances. The graph in Figure 4 displays the ARL_1 values and shift sizes to illustrate the sensitivity performance of the chart, which utilized real-life data from the quarterly durian export volume.

Table 5. ARL_1 values of the explicit formula for the trend $SAR(1)_4$ model on two-sided double EWMA and extended EWMA charts using the dataset of quarterly durian export volume (Unit: 10,000 Metric Tons) for interval [0.01,UCL] with various λ_1 and λ_2, and known parameters; $\eta = 0.1, \omega = 0.6, \phi_1 = 0.5$ at $ARL_0 = 370$.

λ_1	Control Chart	EEWMA		DEWMA			
		EEWMA-1	EEWMA-2	DEWMA-1	DEWMA-2	DEWMA-3	DEWMA-4
	λ_2	$\lambda_2 = 0.2\lambda_1$	$\lambda_2 = 0.8\lambda_1$	$\lambda_2 = 0.6\lambda_1$	$\lambda_2 = \lambda_1$	$\lambda_2 = 2\lambda_1$	$\lambda_2 = 3\lambda_1$
	UCL / δ	0.1922881	0.1632685	0.010770176	0.012335205	0.0173269	0.02277571
	0.0005	290.44	282.04	71.76	144.48	213.56	236.25
	0.001	239.12	227.95	40.15	90.07	150.27	173.67
	0.0025	156.49	144.92	17.76	42.71	79.89	97.08
0.05	0.005	99.58	90.47	9.61	23.16	45.23	56.29
	0.01	58.01	52.01	5.39	12.48	24.59	30.95
	0.05	14.25	12.67	1.94	3.44	6.09	7.53
	0.1	7.89	7.05	1.50	2.28	3.64	4.37
	0.5	2.59	2.38	1.14	1.33	1.62	1.77
	AEQL	0.096	0.088	0.038	0.046	0.058	0.064
	PCI	2.516	2.303	1.000	1.192	1.504	1.666
	RMI	5.853	5.270	0.000	0.981	2.435	3.130
	UCL / δ	0.383444	0.318033	0.0165643	0.0248221	0.0472788	0.0703772
	0.0005	295.01	284.87	216.64	242.65	261.52	267.59
	0.001	245.29	231.52	153.32	180.65	202.28	209.64
	0.0025	163.11	148.45	82.01	102.54	120.69	127.30
0.10	0.005	104.94	93.19	46.53	59.91	72.46	77.23
	0.01	61.59	53.76	25.30	33.05	40.61	43.55
	0.05	15.18	13.10	6.20	7.97	9.76	10.47
	0.1	8.37	7.27	3.66	4.57	5.49	5.86
	0.5	2.68	2.42	1.58	1.78	1.97	2.05
	AEQL	0.100	0.090	0.056	0.064	0.072	0.076
	PCI	1.774	1.592	1.000	1.142	1.284	1.341
	RMI	1.009	0.799	0.000	0.225	0.436	0.516
	UCL / δ	0.584395	0.474338	0.02923571	0.0493974	0.1020756	0.155512
	0.0005	298.10	285.86	249.41	262.34	271.83	274.99
	0.001	249.64	232.97	188.23	203.26	214.90	218.87
	0.0025	167.99	150.03	108.70	121.55	132.20	135.97
	0.005	108.98	94.44	64.08	73.07	80.81	83.63
0.15	0.01	64.35	54.58	35.52	40.97	45.79	47.57
	0.05	15.91	13.31	8.52	9.83	11.01	11.45
	0.1	8.75	7.38	4.83	5.51	6.13	6.36
	0.5	2.75	2.44	1.81	1.96	2.10	2.15
	AEQL	0.103	0.091	0.066	0.072	0.078	0.080
	PCI	1.563	1.373	1.000	1.093	1.177	1.208
	RMI	0.597	0.401	0.000	0.115	0.215	0.251

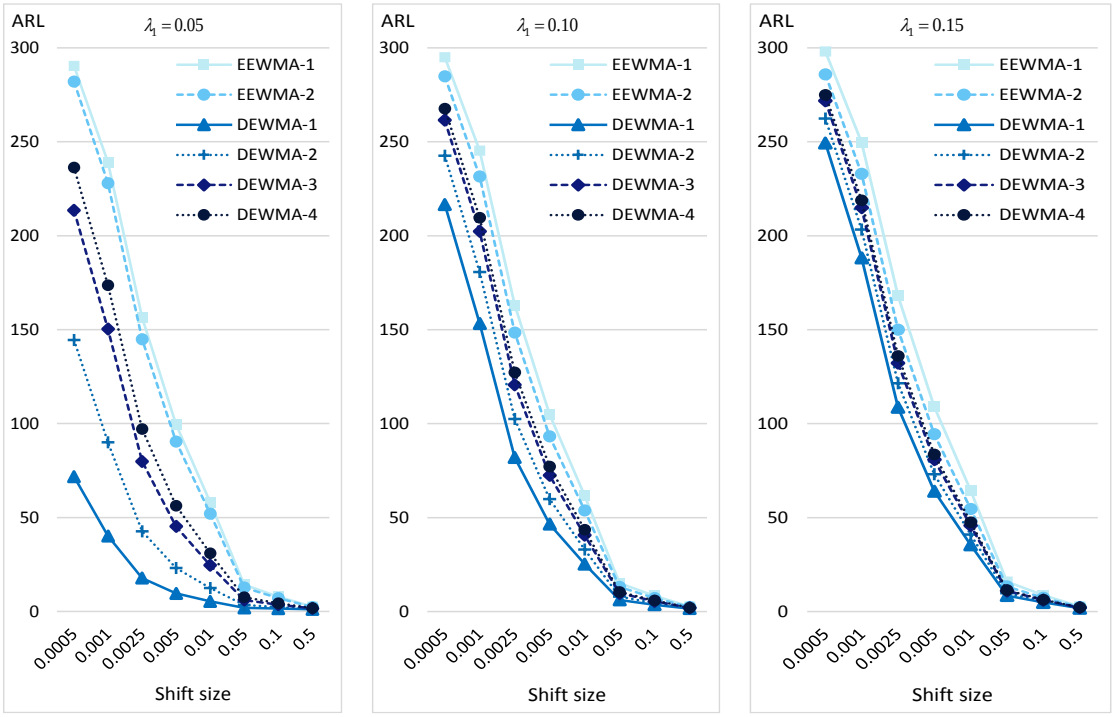

Figure 4. ARL$_1$ values of explicit formula for two-sided double EWMA and extended EWMA charts using the dataset of quarterly durian export volume under various λ_2 with λ_1 equal to (a) 0.05, (b) 0.10, (c) 0.15

The following is how the trend SAR(1)$_{12}$ model was derived:

Dataset 2: Dataset of monthly durian export volume (Unit: 10,000 Metric Tons). It was determined as trend SAR(1)$_{12}$ model, the equation is presented as follows:

$$X_t = 0.063t + 0.693X_{t-12} + \varepsilon_t \tag{32}$$

where; $\varepsilon_t \sim Exp(4.20959)$.

Table 6 also includes the same analysis results as those in Table 5. The results indicate that double EWMA chart ($\lambda_2 = 0.6\lambda_1$), which uses actual data on the volume of monthly durian exports, exhibits superior performance in confirming the consistency of results produced from the simulated data mentioned earlier. Figure 5 is provided to demonstrate the efficacy of double EWMA chart with $\lambda_2 = 0.6\lambda_1$.

Table 6. ARL$_1$ values of the explicit formula for the trend SAR(1)$_{12}$ model on two-sided DEWMA and EEWMA charts using the dataset of monthly durian export volume (Unit: 10,000 Metric Tons) for interval [0.01,UCL] with various λ_1 and λ_2, and known parameters; $\eta = 0.1, \omega = 0.6, \phi_1 = 0.5$ at ARL$_0$ = 370.

λ_1	Control Chart	EEWMA		DEWMA			
		EEWMA-1	EEWMA-2	DEWMA-1	DEWMA-2	DEWMA-3	DEWMA-4
	λ_2	$\lambda_2 = 0.2\lambda_1$	$\lambda_2 = 0.8\lambda_1$	$\lambda_2 = 0.6\lambda_1$	$\lambda_2 = \lambda_1$	$\lambda_2 = 2\lambda_1$	$\lambda_2 = 3\lambda_1$
0.05	δ \ UCL	0.2428652	0.213923	0.011816571	0.014734531	0.02325905	0.0322581
	0.0005	289.25	282.95	118.93	185.11	237.34	253.83
	0.001	237.48	229.01	71.21	123.69	174.83	193.22
	0.0025	154.73	145.92	32.75	62.37	97.98	112.86
	0.005	98.16	91.22	17.64	34.54	56.90	66.99
	0.01	57.06	52.48	9.57	18.64	31.33	37.32
	0.05	13.98	12.78	2.83	4.80	7.65	9.05
	0.1	7.74	7.10	1.97	2.99	4.45	5.16
	0.5	2.54	2.38	1.26	1.50	1.81	1.96

AEQL		0.095	0.088	0.043	0.052	0.065	0.071
PCI		2.199	2.055	1.000	1.218	1.517	1.658
RMI		3.113	2.839	0.000	0.687	1.542	1.920
0.10	UCL / δ	0.486486	0.419822	0.0228677	0.0369392	0.073998	0.111691
	0.0005	293.25	284.86	239.39	258.83	272.57	277.18
	0.001	242.79	231.63	177.00	198.92	215.75	221.55
	0.0025	160.33	148.64	99.63	117.67	132.98	138.51
	0.005	102.65	93.34	57.96	70.31	81.40	85.54
	0.01	60.04	53.87	31.92	39.31	46.18	48.80
	0.05	14.75	13.13	7.73	9.48	11.16	11.81
	0.1	8.14	7.28	4.46	5.36	6.23	6.57
	0.5	2.62	2.42	1.77	1.97	2.16	2.23
AEQL		0.098	0.090	0.064	0.072	0.080	0.083
PCI		1.526	1.401	1.000	1.125	1.245	1.291
RMI		0.633	0.497	0.000	0.171	0.325	0.383
0.15	UCL / δ	0.741923	0.606367	0.0455637	0.0792475	0.1657693	0.253037
	0.0005	295.96	285.87	264.00	273.67	280.94	283.52
	0.001	246.63	232.96	205.20	217.16	226.49	229.77
	0.0025	164.61	150.01	123.24	134.32	143.42	146.67
	0.005	106.17	94.42	74.28	82.40	89.29	91.79
	0.01	62.42	54.57	41.73	46.80	51.21	52.82
	0.05	15.38	13.31	10.04	11.29	12.40	12.82
	0.1	8.46	7.37	5.64	6.29	6.87	7.09
	0.5	2.68	2.43	2.01	2.16	2.29	2.34
AEQL		0.100	0.091	0.074	0.080	0.085	0.087
PCI		1.360	1.225	1.000	1.081	1.152	1.178
RMI		0.369	0.232	0.000	0.091	0.169	0.198

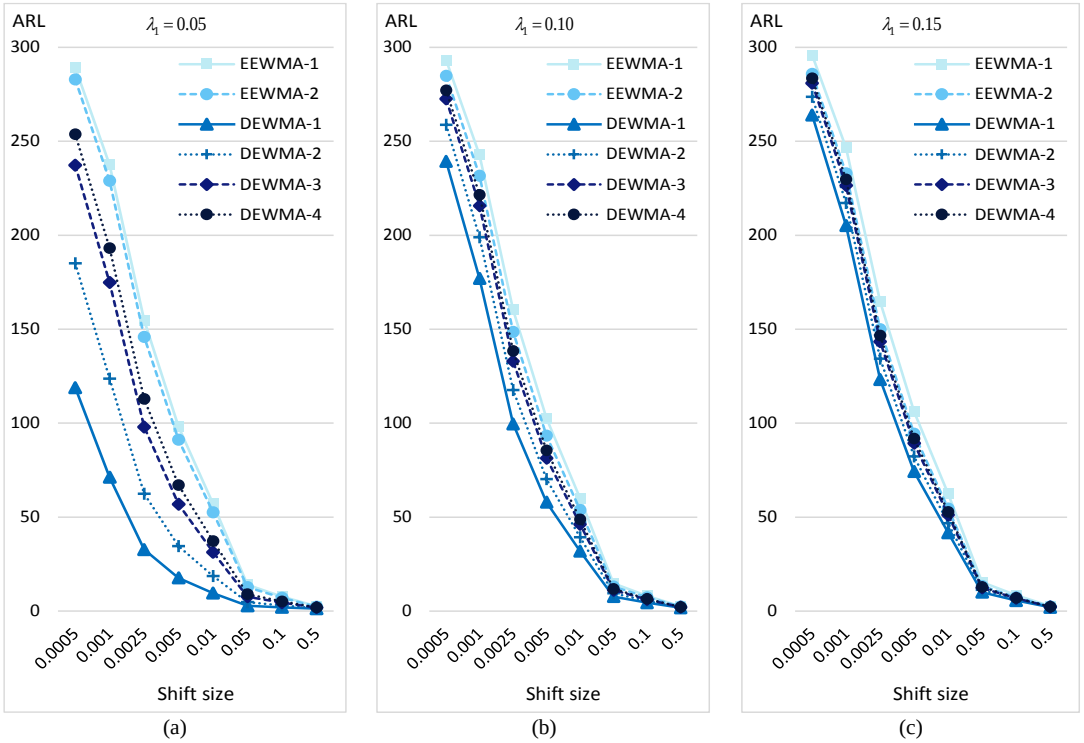

Figure 5. ARL1 values of explicit formula for two-sided double EWMA and extended EWMA charts using the dataset of monthly durian export volume under various λ_2 with λ_1 equal to (a) 0.05, (b) 0.10, (c) 0.15

Consequently, the control chart graphs in Figure 6 show how well they detect process alterations during monitoring using dataset 1: Dataset of quarterly durian export volume in Thailand (Unit: 10,000 Metric Tons). The results show that the double EWMA control chart (with defined $\lambda_1 = 0.05$ and $\lambda_2 = 0.6\lambda_1$), created with the trend SAR(1)$_4$ model, originally with an in-control ARL of 370, indicated the first out-of-control state at the 28th observation. In contrast, the extended EWMA control chart (with defined $\lambda_1 = 0.05$ and $\lambda_2 = 0.8\lambda_1$) signaled the first out-of-control condition at the 40th observation.

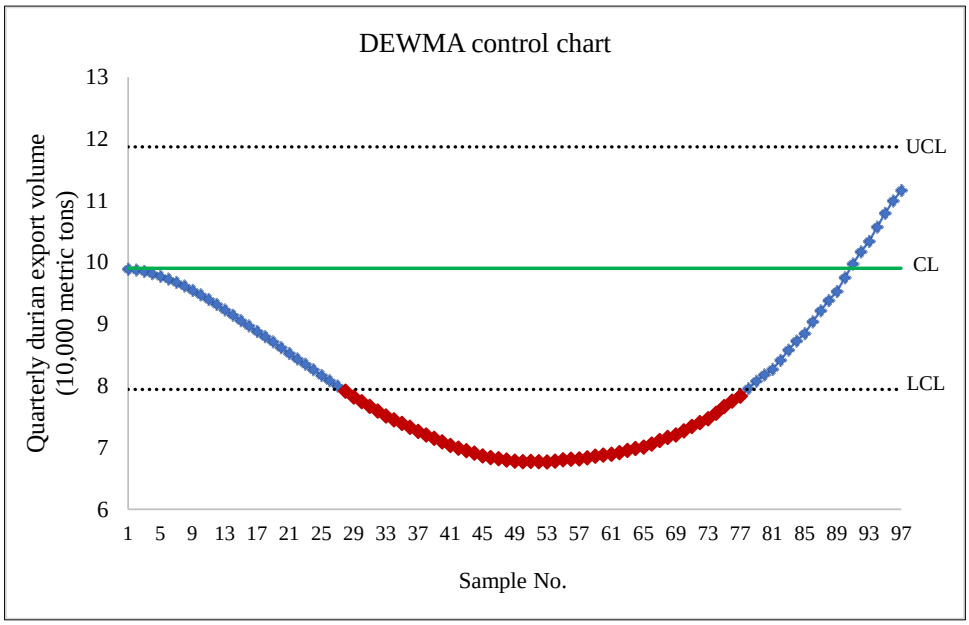

(a)

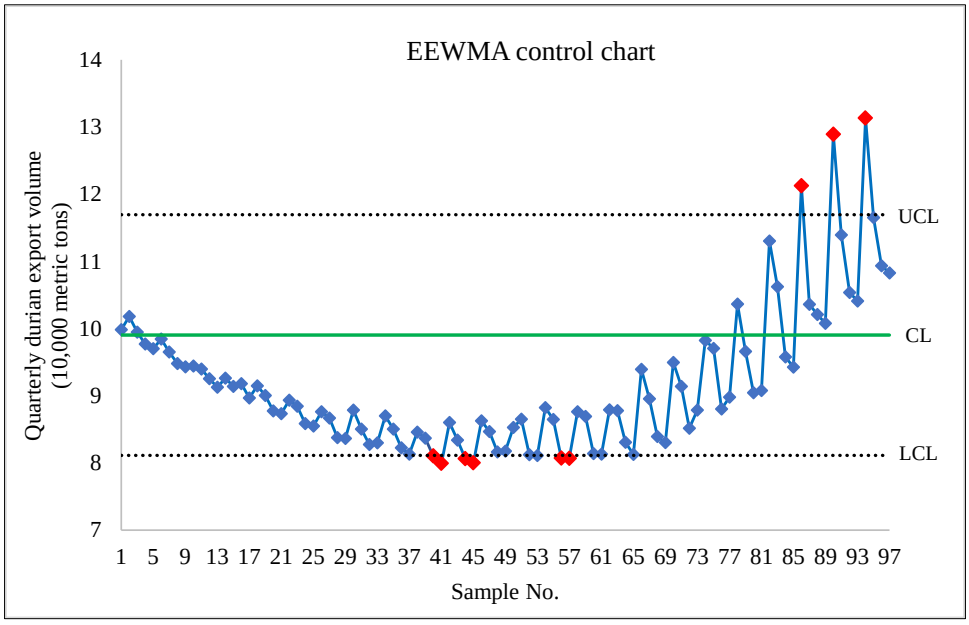

(b)

Figure 6. The sensitivity of detecting processes of two-sided control charts of the dataset of quarterly durian export volume with trend SAR(1)4 under $\lambda_1 = 0.05$ (a) double EWMA (DEWMA) control chart with $\lambda_2 = 0.6\lambda_1$ and (b) extended EWMA (EEWMA) control chart with $\lambda_2 = 0.8\lambda_1$.

While dataset 2: Monthly Durian Export Volume in Thailand (Unit: 10,000 Metric Tons) also used control chart graphs to assess the efficacy of monitoring. The double EWMA chart (with defined $\lambda_1 = 0.05$ and $\lambda_2 = 0.6\lambda_1$), which was created using the trend SAR(1)$_{12}$ model as previously described and initialized with an in-control ARL of 370, appears to have recognized the first out-of-control signal at the 31st observation. The extended EWMA chart (with defined $\lambda_1 = 0.05$ and $\lambda_2 = 0.8\lambda_1$), on the other hand, discovered the shift later, at the 49th observation. The figures that depict these results can be seen in Figure 7.

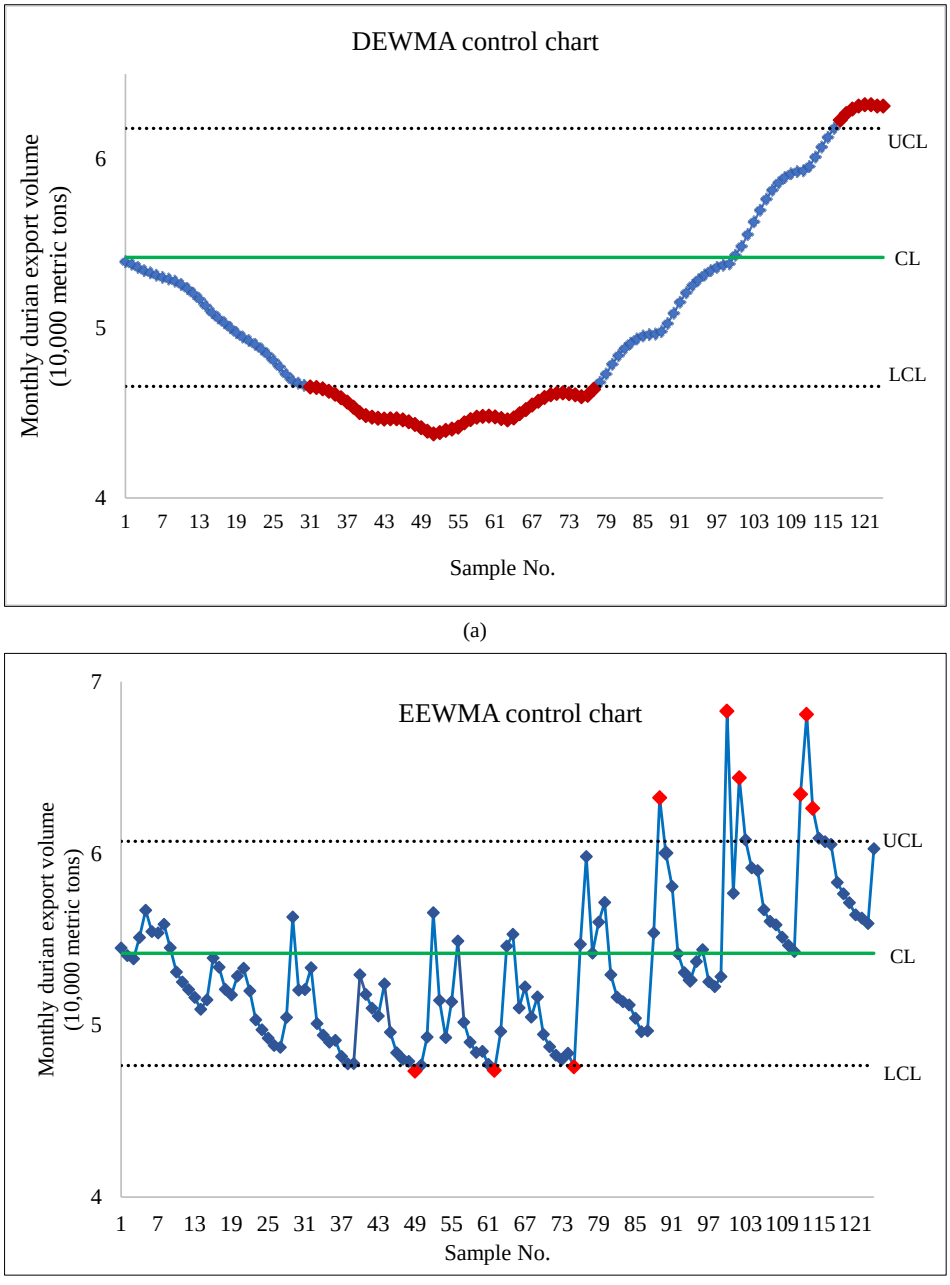

Figure 7. The sensitivity of detecting processes of two-sided control charts of the dataset of monthly durian export volume with trend SAR(1)4 under $\lambda_1 = 0.05$ (a) double EWMA (DEWMA) control chart with $\lambda_2 = 0.6\lambda_1$ and (b) extended EWMA (EEWMA) control chart with $\lambda_2 = 0.8\lambda_1$.

This study's findings indicate that the double EWMA control chart exhibits superior responsiveness compared to the extended EWMA chart in promptly identifying minor process changes, particularly in datasets characterized by autocorrelation.

5- Conclusion

The double EWMA control chart was evaluated using the explicit ARL formula, which exhibited more computing efficiency than NIE methods that depend on four quadrature rules. The trend SAR(1)$_L$ model with exponential white noise yields an accurate solution that matches the ARL accuracy of the NIE technique while significantly enhancing computational speed, rendering it appropriate for real-time and large-scale monitoring. The explicit ARL formula for the double EWMA chart was subsequently compared with the extended EWMA chart under out-of-control scenarios across different shift magnitudes. The evaluation of detection performance utilized sensitivity measures (AEQL, PCI, RMI), demonstrating that both the explicit and NIE methodologies provide very similar ARL results; yet the explicit technique is significantly more rapid (instantaneous compared to 1.5–26 seconds). Although variations in computational environment or parameter settings may lead to minor differences in processing time, these factors do not affect the consistency of ARL accuracy between the explicit and NIE methods.

The results indicate that the double EWMA chart surpasses the extended EWMA chart in identifying process changes in both one-sided and two-sided configurations, especially when lower smoothing settings are utilized. Decreasing the smoothing parameter lowers ARL_1 readings, hence improving detection efficacy. Furthermore, establishing the LCL at 0.005 yielded the greatest sensitivity in detecting process alterations. The results verify the efficacy of the explicit ARL approach, supported by AEQL, PCI, and RMI, along with actual Thai durian export data (monthly and quarterly, in 10,000 metric tons). The suggested technique enhances process monitoring by increasing the sensitivity and speed of shift identification in double EWMA charts.

The present findings are consistent with the previous study by Karoon & Areepong [19], which indicated that the sensitivity performance of the double EWMA control chart based on the trend AR(p) process was superior to that of the traditional EWMA and CUSUM control charts. Nonetheless, this finding establishes the foundation for subsequent endeavors to identify subtle modifications in various data types. Though it might only be effective on autocorrelation datasets using a seasonal autoregressive (SAR) model with a trend component, the exact technique has demonstrated efficacy. This approach might be extended in future research to accommodate more data types with a wider range of properties. Moreover, a limitation of this study is that the evaluation was based on simulated data and durian export series, which may not represent all industrial applications or time-series structures. Future work should extend the analysis to multivariate models and larger datasets to further validate the generalizability of the proposed approach.

6- Declarations

6-1- Author Contributions

Conceptualization, K.K. and Y.A.; methodology, K.K.; software, K.K.; validation, K.K. and Y.A.; formal analysis, K.K.; investigation, Y.A.; resources, K.K.; data curation, K.K.; writing—original draft preparation, K.K.; writing—review and editing, K.K.; visualization, K.K.; supervision, Y.A.; project administration, K.K.; funding acquisition, K.K. All authors have read and agreed to the published version of the manuscript.

6-2- Data Availability Statement

The datasets for monthly and quarterly durian export volumes (in 10,000 metric tons) can be found here: https://app.bot.or.th/BTWS_STAT/statistics/BOTWEBSTAT.aspx?reportID=979&language=TH.

6-3- Funding

This research was funded by Naresuan University under Grant number R2568C028.

6-4- Institutional Review Board Statement

Not applicable.

6-5- Informed Consent Statement

Not applicable.

6-6- Conflicts of Interest

The authors declare that there is no conflict of interest regarding the publication of this manuscript. In addition, the ethical issues, including plagiarism, informed consent, misconduct, data fabrication and/or falsification, double publication and/or submission, and redundancies have been completely observed by the authors.

7- References

[1] Freitas, L. L. G., Kalbusch, A., Henning, E., & Walter, O. M. F. C. (2021). Using statistical control charts to monitor building water consumption: A case study on the replacement of toilets. Water (Switzerland), 13(18), 2474. doi:10.3390/w13182474.

[2] Kovarik, M., & Klimek, P. (2012). The Usage of Time Series Control Charts for Financial Process Analysis. Journal of Competitiveness, 4(3), 29–45. doi:10.7441/joc.2012.03.03.

[3] Khan, N., Aslam, M., Jeyadurga, P., & Balamurali, S. (2021). Monitoring of production of blood components by attribute control chart under indeterminacy. Scientific Reports, 11(1), 922. doi:10.1038/s41598-020-79851-5.

[4] Raza, S. M. M., Sial, M. H., Hassan, N. ul, Mekiso, G. T., Tashkandy, Y. A., Bakr, M. E., & Kumar, A. (2024). Use of improved memory type control charts for monitoring cancer patients recovery time censored data. Scientific Reports, 14(1), 5604. doi:10.1038/s41598-024-55731-0.

[5] Roberts, S. W. (1959). Control Chart Tests Based on Geometric Moving Averages. Technometrics, 1(3), 239–250. doi:10.1080/00401706.1959.10489860.

[6] Page, E. S. (1954). Continuous Inspection Schemes. Biometrika, 41(1–2), 100–115. doi:10.1093/biomet/41.1-2.100.

[7] Naveed, M., Azam, M., Khan, N., & Aslam, M. (2018). Design of a Control Chart Using Extended EWMA Statistic. Technologies, 6(4), 108–122. doi:10.3390/technologies6040108.

[8] Khan, N., Aslam, M., & Jun, C. (2016). Design of a Control Chart Using a Modified EWMA Statistic. Quality and Reliability Engineering International, 33(5), 1095–1104. doi:10.1002/qre.2102.

[9] Shamma, S. E., & Shamma, A. K. (1992). Development and Evaluation of Control Charts Using Double Exponentially Weighted Moving Averages. International Journal of Quality & Reliability Management, 9(6), 18–25. doi:10.1108/02656719210018570.

[10] Mahmoud, M. A., & Woodall, W. H. (2010). An Evaluation of the Double Exponentially Weighted Moving Average Control Chart. Communications in Statistics - Simulation and Computation, 39(5), 933–949. doi:10.1080/03610911003663907.

[11] Ibazizen, M., & Fellag, H. (2003). Bayesian estimation of an AR(1) process with exponential white noise. Statistics, 37(5), 365–372. doi:10.1080/0233188031000078042.

[12] Brook, D., & Evans, D. A. (1972). An approach to the probability distribution of CUSUM run length. Biometrika, 59(3), 539–549. doi:10.1093/biomet/59.3.539.

[13] Champ, C. W., & Rigdon, S. E. (1991). A comparison of the Markov chain and the integral equation approaches for evaluating the run length distribution of quality control charts. Communications in Statistics - Simulation and Computation, 20(1), 191–204. doi:10.1080/03610919108812948.

[14] Peerajit, W. (2023). Developing average run length for monitoring changes in the mean on the presence of long memory under seasonal fractionally integrated MAX model. Mathematics and Statistics, 11(1), 34–50. doi:10.13189/ms.2023.110105.

[15] Supharakonsakun, Y. (2021). Statistical design for monitoring process mean of a modified EWMA control chart based on autocorrelated data. Walailak Journal of Science and Technology, 18(12), 19813. doi:10.48048/wjst.2021.19813.

[16] Ng, P. S., Goh, S. Y., Saha, S., & Yeong, W. C. (2021, April). An enhanced double EWMA chart for monitoring the process mean shifts. International Conference on Robotics, Vision, Signal Processing and Power Applications, Springer Nature, Singapore. doi:10.1007/978-981-99-9005-4_48.

[17] Capizzi, G., & Masarotto, G. (2003). An adaptive exponentially weighted moving average control chart. Technometrics, 45(3), 199-207. doi:10.1198/004017003000000023.

[18] Karoon, K., Areepong, Y., & Sukparungsee, S. (2023). Modification of ARL for detecting changes on the double EWMA chart in time series data with the autoregressive model. Connection Science, 35(1), 2219040. doi:10.1080/09540091.2023.2219040.

[19] Horng Shiau, J. J., & Ya-Chen, H. (2005). Robustness of the EWMA control chart to non-normality for autocorrelated processes. Quality Technology & Quantitative Management, 2(2), 125-146.doi:10.1080/16843703.2005.11673089.

[20] Bualuang, D., & Peerajit, W. (2022). Performance of the CUSUM Control Chart Using Approximation to ARL for Long-Memory Fractionally Integrated Autoregressive Process with Exogenous Variable. Applied Science and Engineering Progress, 16(2), 5917. doi:10.14416/j.asep.2022.05.003.

[21] Karoon, K., & Areepong, Y. (2024). Enhancing the Performance of an Adjusted MEWMA Control Chart Running on Trend and Quadratic Trend Autoregressive Models. Lobachevskii Journal of Mathematics, 45(4), 1601-1617. doi:10.1134/S1995080224601577.

[22] Muangngam, T., Areepong, Y., & Sukparungsee, S. (2024). Performance Evaluation of Extended EWMA Chart for AR Model with Exogenous Variables. HighTech and Innovation Journal, 5(4), 901–917. doi:10.28991/HIJ-2024-05-04-03.

[23] Sunthornwat, R., Sukparungsee, S., & Areepong, Y. (2024). The Development and Evaluation of Homogenously Weighted Moving Average Control Chart based on an Autoregressive Process. HighTech and Innovation Journal, 5(1), 16–35. doi:10.28991/HIJ-2024-05-01-02.

[24] Karoon, K., & Areepong, Y. (2025). The Efficiency of the New Extended EWMA Control Chart for Detecting Changes Under an Autoregressive Model and Its Application. Symmetry, 17(1), 104. doi:10.3390/sym17010104.

[25] Peerajit, W. (2025). Optimizing the EWMA Control Chart to Detect Changes in the Mean of a Long-Memory Seasonal Fractionally Integrated Moving Average and an Exogenous Variable Process with Exponential White Noise and its Application to Electrical Output Data. WSEAS Transactions on Systems and Control, 20, 25–41. doi:10.37394/23203.2025.20.4.

[26] Polyeam, D., & Phanyaem, S. (2025). Enhancing Average Run Length Efficiency of the Exponentially Weighted Moving Average Control Chart under the SAR(1)L Model with Quadratic Trend. Malaysian Journal of Fundamental and Applied Sciences, 21(3), 2174–2193. doi:10.11113/mjfas.v21n3.4290.

[27] Polyeam, D., & Phanyaem, S. (2025). Application of EWMA Control Chart for Analyzing Changes in SAR(P)L Model with Quadratic Trend. Mathematics and Statistics, 13(3), 163–174. doi:10.13189/ms.2025.130305.

[28] Almousa, M. (2020). Adomian Decomposition Method with Modified Bernstein Polynomials for Solving Nonlinear Fredholm and Volterra Integral Equations. Mathematics and Statistics, 8(3), 278–285. doi:10.13189/ms.2020.080305.

[29] Sofonea, M., Han, W., & Shillor, M. (2005). Analysis and Approximation of Contact Problems with Adhesion or Damage. Chapman and Hall/CRC, Boca Raton, United States. doi:10.1201/9781420034837.